Kinetic Study on Heavy Metal Divalent Ions Removal using Zirconium-Based Magnetic Sorbent

Article · March 2020

DOI: 10.30880/ijie.2020.12.03.026

© Universiti Tun Hussein Onn Malaysia Publisher's Office

IJIE

Journal homepage: http://penerbit.uthm.edu.my/ojs/index.php/ijie
ISSN : 2229-838X e-ISSN : 2600-7916

The International Journal of Integrated Engineering

Kinetic Study on Heavy Metal Divalent Ions Removal using Zirconium-Based Magnetic Sorbent

S. F. Lim[1,*], A. Y. W. Lee[1], S. N. D. Chua[1], B. H. Lim[2], Pushpdant Jain[3]

[1]Faculty of Engineering, Universiti Malaysia Sarawak, 94300, Kota Samarahan, Sarawak, MALAYSIA

[2]Faculty of Engineering and Information Technology, Mahsa University, 42610 Jenjarom, Selangor, MALAYSIA

[3]Department of Mechanical Engineering, Oriental Institute of Science and Technology, 462021 Bhopal, INDIA

*Corresponding Author

DOI: https://doi.org/10.30880/ijie.2020.12.03.026
Received 18 December 2019; Accepted 14 January 2020; Available online 30 February 2020

Abstract: In this research, zirconium-based magnetic sorbent synthesised by chemical co-precipitation method is explored as a potential sorbent for removal of divalent metal ions from aqueous solution. The interaction characteristics between the ions and the sorbent were elucidated by instrumental analyses such as Fourier Transform InfraRed (FT-IR) Spectroscopy, Scanning Electron Microscopy (SEM), and Brunauer, Emmett, and Teller (BET) surface area analyser. Results show that the sorption rate was increased with an increase in contact time and initial metal ion concentration. Moreover, a two-stage kinetics behaviour was observed, and all the batch experiments achieved an equilibrium state within 4 hours. The evaluation of the adsorption behaviour of heavy metal divalent ions onto the magnetic sorbent was explained using two kinetic models, and it was mostly found to follow the postulate of the pseudo-second-order kinetic model. The validity of kinetic models applied in this study is also evaluated by using a normalised standard deviation.

Keywords: Zirconium based magnetic, FTIR, BET

1. Introduction

In recent years, the speedy development has increased the severity of the environmental pollution problems and heavy metal contamination of industrial water is a significant universal problem. There is a growing number of contaminants which enter water supplies from human activities in both developing and industrialized nations [1]. Many countries discharged the effluent to surface water without any treatment because of technological and economical limitations [2], [3]. Chu et al. [4] stated that most heavy metals are well-documented as toxic and carcinogenic agents. The potentially toxic and relatively accessible metals including copper (Cu), zinc (Zn), and cadmium (Cd) has attracted the keen attention of the researchers [4],[5]. The existence of these heavy metals in the atmosphere, soil, and water is a threat to all organisms even in traces; especially the bioaccumulation in the food chain can be extremely hazardous to human health [5]. In the same manner, discharge of the heavy metal into wastewater poses serious threat to the human population, fauna and flora of the receiving water bodies [6].

Over the past two decades, environmental regulations have become more stringent, requiring an improved quality of treated effluent. In fact, industrial wastewater varies considerably in their nature, toxicity, and treatability [7]. Comparatively, the prevalence of adsorption separation in the environmental chemistry remains an aesthetic attention and consideration abroad the nations, owning to its low initial cost, simplicity of design, ease of operation, insensitivity to toxic substances, and complete removal of pollutants even from dilute solutions.

*Corresponding author: sflim@unimas.my

Furthermore, separation and recovery of adsorbents from the decontaminated water can be tremendously challenging [8]. Magnetic sorption technology is one of the treatment processes that received considerable attention from researchers because magnetic sorbent can be separated easily from solution after treatment while fewer secondary wastes are produced.

Nomenclatures:

C_0	Initial heavy metal ions concentration, mg/L
C_t	Heavy metal ions concentration at given time t, mg/L
c	Weber-Morris diffusion intercept
k	Pseudo-second-order rate constants, mg/g min
k_{id}	Intra-particle diffusion rate constant, mg/g min
n	Number of data points
q_e	Adsorption capacity at equilibrium, mg/g
q_t	Adsorption capacity at time t, mg/g
$q_{t,cal}$	Calculated adsorption uptake at time t, mg/g
$q_{t,exp}$	Experimental adsorption uptake at time t, mg/g
Δq	Normalized standard deviation, %
R^2	Correlation coefficient
t	Time, min
V	Volume of the heavy metal ions solutions, mL
W	Weight of magnetic sorbent, mg

Abbreviations

AAS	Atomic Absorption Spectrophotometer
ATR	Attenuated total reflectance
BET	Brunauer, Emmett, and Teller
FAE	Fractional attainment of equilibrium
FT-IR	Fourier Transform InfraRed Spectroscopy
SEM	Scanning Electron Microscopy

Based on some reported magnetic sorbents with their applications in environmental and chemical engineering fields, poly(1-vinylimidazole)-grafted magnetic (maghemite, ɣ-Fe_2O_3) nanoparticles showed selective binding of divalent ions in the following order: $Cu^{2+} > Ni^{2+} > Co^{2+}$ [9]. A natural biodegradable and renewable resin with abundant hydroxyl and carboxylic groups was used as a coating layer on the surface of iron oxide magnetic nano-material and reported as a newly synthesized effective adsorbent for removal of cadmium from aqueous solution [10]. The present work aims to synthesize a zirconium-based magnetic sorbent for adsorptive removal of heavy metal ions from synthetic aqueous solution. The study evaluates the potential of the magnetic sorbent for the removal of aqueous contaminants, Cu^{2+}, Zn^{2+}, and Cd^{2+} as divalent ion selectivity is generally much higher than that for monovalent ions besides the sorption of monovalent ions is usually non-specific [11]. In addition, zirconium has received increasing attention and demonstrated to remove anionic contaminants from aqueous solution successfully; hence the sorption capacity for cationic contaminant is also examined in this study. The sorbent aforementioned with better magnetic properties, lower toxicity, and lower price could be easily collected with a high gradient magnet and possessed favourable adsorption capacity for heavy metal ions. Confirmatory tests using Scanning Electron Microscopy (SEM) and instrumental analyses of Fourier Transform InfraRed (FT-IR) Spectroscopy, and Brunauer, Emmett, and Teller (BET) surface area analyser to study the properties are reported. Other than that, kinetics of heavy metal ions removal was determined in order to elucidate a possible ion exchange mechanism between zirconium-iron oxide particles and heavy metal ions in aqueous solution as well as modelling the processes.

2. Materials and methods

2.1 Materials

All chemicals used were of analytical reagent grade and used without further purification. The raw materials for the synthesis of sorbent, zirconium (IV) sulfate ($Zr(SO_4)_2$), iron (II) chloride ($FeCl_2 \cdot 4H_2O$), and iron (III) chloride ($FeCl_3 \cdot 6H_2O$) were obtained from Sigma-Aldrich Co. LLC whereas sodium hydroxide (NaOH) was obtained from Merck. The adsorbates, copper (II) sulfate ($CuSO_4 \cdot 5H_2O$), zinc sulfate ($ZnSO_4 \cdot 7H_2O$), and cadmium nitrate ($Cd(NO_3)_2 \cdot 4H_2O$) were purchased from Fisher Scientific UK Ltd. The stock solution of Cu^{2+}, Zn^{2+}, and Cd^{2+} were prepared by dissolving $CuSO_4 \cdot 5H_2O$, $ZnSO_4 \cdot 7H_2O$, and $Cd(NO_3)_2 \cdot 4H_2O$ in appropriate amounts of ultrapure water produced using Sartorius arium® pro ultrapure water system. All working solutions were freshly prepared by diluting the stock solutions to the desired concentrations, and pH was adjusted to the desired values with hydrochloric acid

(HCl) and sodium hydroxide (NaOH) solutions. The pH measurements were made using an Accumet AB15 pH meter equipped with a combine electrode (Fisher Scientific, USA).

2.2 Synthesis of magnetic sorbent

The zirconium-based magnetic sorbent was synthesized according to the Lim [12] and Zheng et al. [13] chemical co-precipitation method. 0.4 M of $FeCl_2 \cdot 4H_2O$ and 0.8 M of $FeCl_3 \cdot 6H_2O$ (1:2) were dissolved in ultrapure water. 0.25 M of zirconium sulfate solution was then injected into the mixed solution. The mixture was mechanically stirred with a Memmert water bath (Model WNE 14) and heated to 70 ^{0}C. When the temperature was stabilized, 10 M of NaOH was added drop-wisely until the pH was above 8. Fe-Zr oxides were formed as the precipitate. The precipitate was washed until the pH of supernatant reached approximately 7. The precipitate was separated by magnetic decantation and dried in an oven (BINDER ED 53, Germany) at 70 ^{0}C for 24 h. Finally, the obtained Fe-Zr sorbent was cooled at room temperature. The product was then ground in an agate mortar, appeared in the form of fine powders, subsequently sieved with a 500 µm stainless steel sieve, and kept at desiccator for further use.

2.2 Instrumental analyses

The vibration frequency changes in the virgin zirconium-iron oxide particles and zirconium-iron oxide particles loaded with heavy metals due to the sorption were analysed by Fourier Transform InfraRed (FT-IR) Spectroscopy (Shimadzu IRAffinity-1, Japan) with an attenuated total reflectance (ATR) technique. Samples were measured by pressing them against a diamond prism that is positioned horizontally for the infrared microscope analysis and the infrared spectra were recorded in the IR wavelength between 4000 and 400 cm^{-1}. The spectra data was collected with twenty scans at a resolution of 4 cm^{-1} and the apodization function was of the Happ-Genzel type. All the spectra were recorded and plotted in the same scale on the transmittance axis.

The surface morphology of the synthesized zirconium-based magnetic sorbent were characterized by a JEOL JSM-6390LA Scanning Electron Microscopy (SEM). The dry samples were mounted on aluminium plates using double-sided conductive carbon tape and sputter-coated with an Au film in vacuum using an auto fine coater (JFC-1600, JEOL) prior to measurement. The coated samples were then visualized and examined with the Scanning Electron Microscopy analysis operated at 10 kV. The Brunauer, Emmett and Teller (BET) surface area, average pore radius, and total pore volume of the zirconium-based magnetic sorbent were determined by standard multipoint techniques of N_2 adsorption/desorption, using Autosorb iQ (Quantachrome Instrument, USA) at the temperature of 77 K and were analysed using ASIQwin software. The samples were degassed at 50 ^{0}C for 12 hours in vacuum prior to analysis to remove any adsorbed moisture or other impurities bounded to the surface of the samples.

2.3 Experimental sorption kinetic studies

Experimental kinetic study was conducted in batch mode by varying initial concentration of the heavy metal ions. The study was carried out in a series of Erlenmeyer flasks of 100 mL capacity by agitating the sorbent in the aqueous Cu^{2+}, Zn^{2+}, and Cd^{2+} solutions when pre-determined temperature (25 ± 1 ^{0}C) was attained. The solid-solution ratio was 1:1. The sorption process was performed at a pre-determined time interval using a refrigerated incubating shaker (Thermo Scientific 491, Japan) at constant agitation rate of 200 rpm. The initial concentration of Cu^{2+}, Zn^{2+}, and Cd^{2+} was varied from 20 to 100 mg/L. Flasks were kept sealed in order to minimize losses to atmosphere. After the reaction period, the sorbents were isolated from the medium by the technique of magnetic separation and dried overnight in an oven at 70 ^{0}C prior to instrumental analyses. The solvents were filtered by 0.45 µm membrane filters and analysed for heavy metal ions using the Atomic Absorption Spectrophotometer (AAS) (Shimadzu, AA-7000, Japan). The tests were performed in triplicate for each input concentration C_0 in order to better understand the system. Concentration of Cu^{2+}, Zn^{2+}, and Cd^{2+} on the sorbent was obtained by material balance. The quantity of sorbed heavy metal ions in mg/g at time t was computed by using Eq. (1):

$$q_t = \frac{(C_0 - C_t)V}{W} \quad (1)$$

where C_0 and C_t are the heavy metal ions concentrations in mg/L initially and at given time t, respectively, V is the volume of the heavy metal ions solutions in mL and W is the weight of magnetic sorbent in mg.

3. Results and discussion

3.1. Effect of contact time and initial metal ion concentration

The present study has examined the uptake of Cu^{2+}, Zn^{2+}, and Cd^{2+} for the zirconium-based magnetic sorbent on the variation of initial concentrations at regular time intervals, as illustrated in Fig. 1. The sorption experiments to evaluate the contact time effect on heavy metal ions removal by the magnetic sorbent using AAS were carried out ranging from

0 to 6 h where further increase in contact time did not enhance the adsorption uptake. From Fig. 1, a two-stage kinetics behaviour was observed. The trends were composed of two terms: a fast initial removal (in the first 60 min of treatment) and a slower subsequent removal up to equilibrium state, which was obtained after 240 min of treatment. At the point of equilibrium, the amount of heavy metal ions adsorbed was in equilibrium with the amount of heavy metal ions desorbed.

It was obvious that the amount of sorbed heavy metal ions on the magnetic sorbents increased with an increase in time. The maximum adsorption takes place at 120, 240, and 180 min contact time for Cu^{2+}, Zn^{2+}, and Cd^{2+}, respectively. The equilibrium was reached after the contact period mentioned.

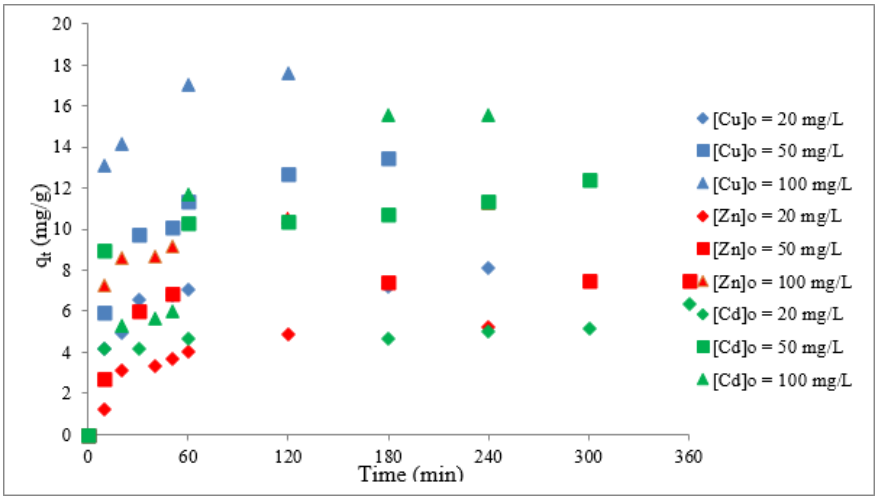

Fig. 1 - Effect of contact time and initial concentration on the removal of Cu^{2+}, Zn^{2+}, and Cd^{2+} by the zirconium-based magnetic sorbent [Experimental conditions: pH = 5, sorbent dosage = 1 g/L, temperature = 25 ^{0}C]

The initial fast sorption might be due to the exchange of micro-scale particle size of sorbents on the surface of sorbents. Fine particles were favourable for the diffusion of heavy metal ions from bulk solution onto the active sites of the sorbents. Moreover, the initial rapid sorption of heavy metal ions could be attributed to the greater vacant binding sites which were available for sorption at the initial stages. The increase in driving force due to the concentration gradient that existed between the adsorbate in solution and the surface of the synthesized zirconium-based magnetic sorbent has contributed to the higher the initial sorption uptake [14,15]. As time proceeded, the heavy metal ions uptake rate by magnetic sorbent was decreased significantly due to the decrease in number of sorption sites as well as ions concentration. The limited mass transfer of the adsorbate molecules due to the accumulation of the sorbed heavy metal ions on sorbent surface has resulted in the decrease of sorption rate. Equilibrium was reached at a later time as a result of slower internal mass transfer within the sorbent particles since the remaining active sites with lower affinities are occupied slowly.

Furthermore, a close look at Fig. 1 has revealed that at equilibrium, unit sorption increased from 8.1 mg/g to 17.6 mg/g, 5.2 mg/g to 11.3 mg/g, and 6.4 mg/g to 15.5 mg/g as the concentration increased from 20 mg/L to 100 mg/L for Cu^{2+}, Zn^{2+}, and Cd^{2+}, respectively. This is because the mass transfer driving force would become larger as the initial concentration increased. Hence, it results in higher heavy metal ions sorption. Apart from that, the Cu^{2+} possessed higher adsorption capacity than Zn^{2+} and Cd^{2+} in most agitation periods. This could be explained that more specific surface area was obtained for Cu^{2+} due to the microporous structure and formation of zirconium-iron oxide particles as Cu^{2+} has a higher tendency to adsorb and form organic complexes than Zn^{2+} and Cd^{2+} [16].

3.2. Characterization of sorbent

3.2.1. Spectroscopic analysis

The surface functional groups of the magnetic sorbents are shown in Fig. 2. The obvious absorption bands at low frequency zone of 500-700 cm^{-1} observed in sorbents are due to metal oxygen stretching vibration. The sharp bands in the range were caused by various lattice vibrations associated with metal hydroxide sheets [17]. This could be due to the presence of Fe-O stretching vibration bond in the magnetic sorbent. In addition, the Fe-O stretching vibration band of the bulk magnetite is usually at ~570 cm^{-1}, and the band has a slight shift to high wavenumbers due to the finite size of particles. A noticeable feature observed from the spectra before and after heavy metal sorption is new peaks at 792 cm^{-1} and 896 cm^{-1} which can be assigned to Fe-O-H bending and stretching vibrations, respectively. These imply that the -OH groups are involved during the metal ions sorption.

In this study, the shoulder at 3367 cm^{-1} can be assigned to the stretching mode of H_2O molecules, whereas the shoulder at 3169 cm^{-1} can be assigned to the stretching mode of the OH group in a goethite structure. Compared with spectrum of zirconium-iron oxide particles before heavy metals adsorption, the peaks were weakened and shifted after heavy metal ions are adsorbed onto the surface of sorbent. The decrease in wavenumber of the peak due to the change in intramolecular hydrogen bonding interactions was attributed to the attachment of heavy metal ions on -OH group [18]. Moreover, the IR band at ~1633 cm^{-1} was due to the bending mode of interlayer H_2O molecules. The OH bending band also can be observed at 1122 cm^{-1} from Figs. 2(b) and (c).

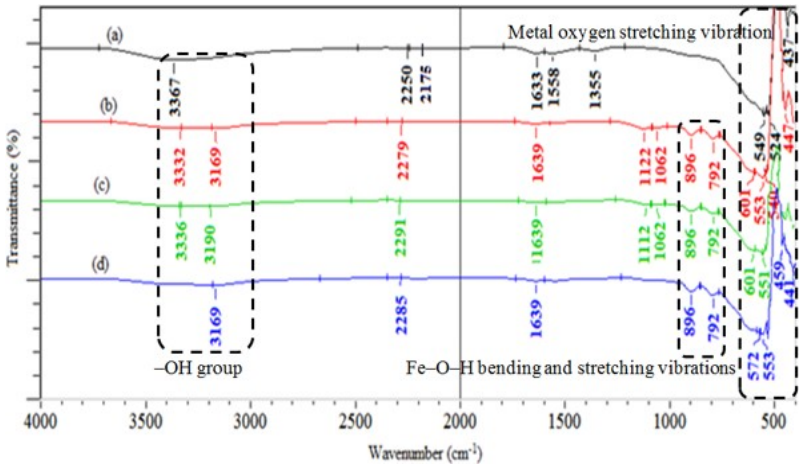

Fig. 2 - FT-IR spectra of the magnetic sorbent (a) before and after sorption of (b) Cu2+, (c) Zn2+, and (d) Cd2+ at the maximum sorption capacity [Experimental conditions: pH = 5, initial concentration = 100 mg/L]

3.2.2 Scanning Electron Microscopy

The morphological characteristics of the magnetic sorbent, before and after sorption process, were illustrated in Fig. 3. It is apparent from these micrographs that the sorbent particles with varying sizes were agglomerated together appearing with irregular surface morphology and have a chalky consistency. As presented in Fig. 3(a), the micrographs obtained for the sorbent showed that the material was constituted by many aggregated small particles, leading to a rough surface and the presence of porous structure. The small particles were merged together giving large agglomerates.

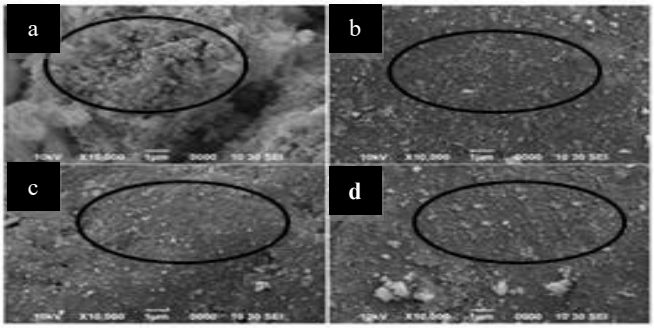

Fig. 3 - SEM micrographs of the zirconium-based magnetic sorbent before and after heavy metal ion adsorption: (a) virgin sorbent, (b) sorbent loaded with Cu^{2+}, (c) sorbent loaded with Zn^{2+}, and (d) sorbent loaded with Cd^{2+} (X10000) [Experimental conditions: pH = 5, initial concentration = 100 mg/L]

The surface of sorbent is rough with abundant protuberance, which might be the magnetite agglomeration [19]. The roughness of the micron-sized magnetic particle surfaces suggested that the irregularly shaped amorphous particles of the magnetic sorbent are similar to the characteristic of zirconia [20]. Additionally, the uneven surface with lots of pores facilitates the diffusion of heavy metal ions into the magnetic sorbent and thereby greatly *promoting* the sorption performance of the *sorbent*.

A clear demarcation in the surface morphology of the sorbent after sorption was observed from Figs. 3(b) - (d). As demonstrated in these figures, the SEM images of sorbent loaded with Cu, Zn, and Cd ions were taken at a magnification capacity of ×10000 and a scale bar of 1 μm. The particle surfaces appear to be smooth and typical of a not well-crystallized material after the sorption process. This indicated that the pores may significantly contribute to the

transfer of metal ions to the surface of the magnetic sorbent. After metal ions sorption, metal ions might be deposited on the sorbent layer and the pores were adhered by the metal ions studied [21,22]. It was also observed that interaction with the metal ions led to the formation of discrete aggregates on the sorbents surface.

3.2.3 Surface area and porosity analysis

The BET surface area and porosity of the zirconium-based magnetic sorbent were estimated from nitrogen adsorption-desorption isotherms. The comparison of the BET surface area, average pore radius, and total pore volume of the sorbent before and after adsorption are summarized in Table 1.

Table 1 - BET surface area and porosity analysis of the sorbent before and after sorption process at the maximum adsorption capacity

Zirconium-based magnetic sorbent	BET surface area (m^2/g)	Average pore radius (nm)	Total pore volume (mL/g)
Virgin sorbent	116.099	0.8051	0.0467
Sorbent loaded with Cu^{2+}	84.252	0.6754	0.0285
Sorbent loaded with Zn^{2+}	94.843	0.7665	0.0391
Sorbent loaded with Cd^{2+}	90.152	0.7340	0.0331

*Note: The zirconium-based magnetic sorbents were loaded with Cu^{2+}, Zn^{2+}, and Cd^{2+} under experimental conditions: pH = 5, initial concentration = 100 mg/L.

A distinct decrease of the average pore radius and total pore volume of the sorbents after adsorption was observed, which is reflected in the surface morphology study by SEM analyses as stated in the previous section. It was suggested that the decrease in total adsorption surface area available to heavy metal ions was resulting from overlapping or aggregation of adsorption sites. Therefore, it can be concluded that the heavy metal ions were adsorbed onto the surface of sorbent throughout the introduced dosage of the sorbent.

3.3 Analysis of sorption kinetics

In order to elucidate the potential rate determining step between zirconium-iron oxide particles and heavy metal ions in aqueous solution, the adsorption kinetics of the removal of the divalent ions by the magnetic sorbent was modelled using several kinetic models including pseudo-first-order, pseudo-second-order, Elovich, Weber-Morris diffusion, fractional attainment of equilibrium (FAE), and liquid film diffusion. The applicability of pseudo-second-order and Weber-Morris diffusion kinetic models is desirable to be presented for the kinetic analysis.

3.3.1 Pseudo-second-order kinetic model

The pseudo-second-order kinetic model based on Eq. (2) is usually represented by its linear form [23], as presented in Fig. 4.

$$\frac{t}{q_t} = \frac{1}{kq_e^2} + \frac{1}{q_e t} \tag{2}$$

where the second order constants k (mg/g min) can be determined experimentally from the slope and intercept of plot t/q_t versus t. Fitted pseudo-second-order model kinetic parameters for the removal of the heavy metal ions by the zirconium-based magnetic sorbent at various initial metal ion concentrations are listed in Table 2. The corresponding linear regression correlation coefficients for the plots of t/q_t against t from the pseudo-second order rate law are incredibly high ($R^2 \geq 0.894$) for all systems. The higher R^2 values confirm that the sorption data were well represented by pseudo-second-order kinetics. Besides, the rate of sorption was found to conform with excellent correlation to pseudo-second-order kinetics.

By comparing the experimental equilibrium concentrations, q_e with those calculated, a good agreement can be observed. This observation made clear that the sorption system is pseudo-second-order model based on the assumption that the chemisorption mechanism as the rate-controlling step, involving valence forces through sharing or exchange of electrons between sorbent and adsorbate [14]. It is suggested that metal ion adsorption onto the zirconium-based magnetic sorbent involves chemisorption, which has been discussed in details in the FT-IR study.

3.3.2 Weber-Morris diffusion kinetic model

In order to have an understanding of the rate-determining step, the Weber and Morris model, namely the intra-particle diffusion model, as Eq. (3) was employed:

$$q = k_{id}t^{1/2} + c \tag{3}$$

where k_{id} is the intra-particle diffusion rate constant (mg/g min) and c is the intercept in the plot of q_t against $t^{1/2}$ that related to the thickness of the boundary layer, indicating the larger the intercept, the higher the contribution of the surface sorption in the rate-controlling step.

Figure 5 depicts the model plots of the experimental data where the values of k_{id} were obtained from the slope of the plots of q_t versus $t^{1/2}$ for various initial metal concentrations. It was observed that for all the metal ions studied, a positive and significant ordinate intercept is obtained, demonstrating the influence of external rate control and the k_{id} values (Table 2) increased with initial metal concentration. An increase in initial concentration has promoted the pore diffusion in sorbent particles and resulted in an enhancement in the intra-particle diffusion rate. It is likely that a large number of ions diffuse into the pore before being adsorbed.

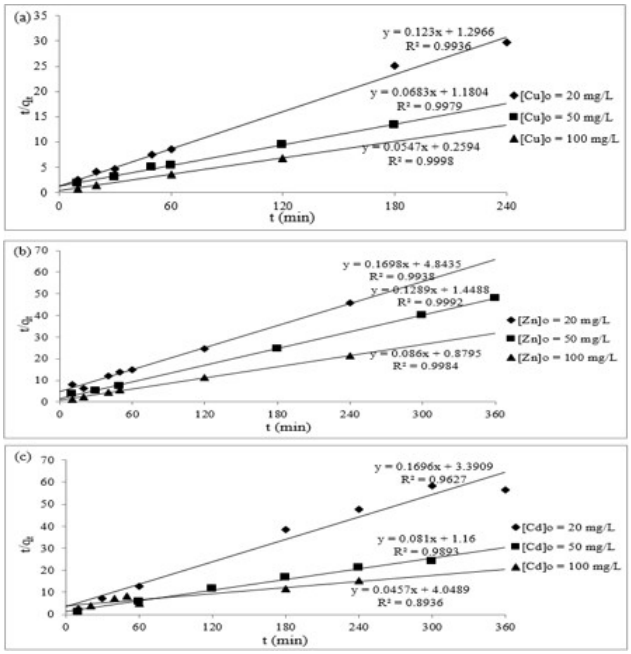

Fig. 4 - Pseudo-second-order plot of the effect of initial concentration on the sorption of heavy metal ions: (a) Cu^{2+}, (b) Zn^{2+}, and (c) Cd^{2+} by using the zirconium-based magnetic sorbent [Experimental conditions: pH = 5, sorbent dosage = 1 g/L, temperature = 25 ^{0}C]

Table 2 - Comparison of kinetic model parameters for sorption of the Cu^{2+}, Zn^{2+}, and Cd^{2+} by using the zirconium-based magnetic sorbent.

Kinetic Models	Para-meter	Copper (Cu)			Zinc (Zn)			Cadmium (Cd)		
		20mg/L	50mg/L	100mg/L	20mg/L	50mg/L	100mg/L	20mg/L	50mg/L	100mg/L
Pseudo-second-order	q_e (exp)	8.095	13.495	17.595	5.232	7.485	11.250	6.387	12.394	15.544
	q_e	8.130	14.641	18.282	5.889	7.758	11.628	5.896	12.346	21.882
	K	0.012	0.004	0.012	0.006	0.012	0.008	0.009	0.006	0.001
Weber-Morris diffusion	k_{id}	0.415	0.965	1.451	0.343	0.333	0.598	0.213	0.379	1.067

According to this model, the plot of q_t versus $t^{1/2}$ should be linear if intra-particle diffusion is involved in the sorption process and if these lines pass through the origin then intra-particle diffusion is the rate-controlling step [24]. It was noticed from Fig. 5 that the plots were not linear over the whole-time range and the straight lines did not pass through the origin. When the plots do not pass through the origin, this is indicative of some degree of boundary layer control. This further shows that the intra-particle diffusion is not the only rate-limiting step, but also other kinetic models may control the rate of adsorption, all of which may be functioning simultaneously.

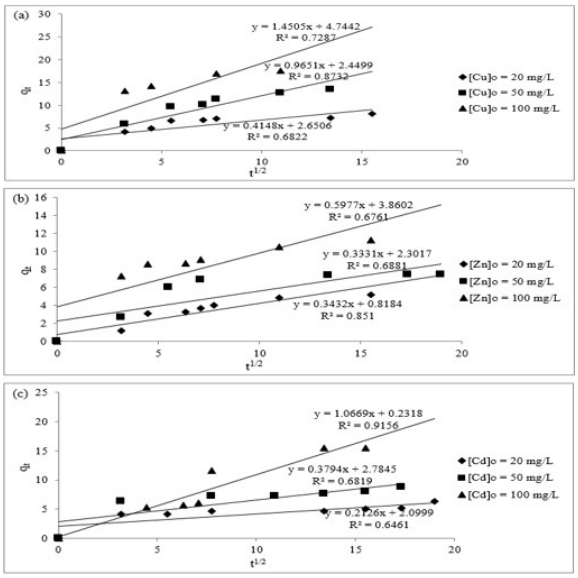

Fig. 5 - Weber-Morris diffusion kinetic model effect on the sorption of heavy metal ions: (a) Cu^{2+}, (b) Zn^{2+}, and (c) Cd^{2+} by using the zirconium-based magnetic sorbent [Experimental conditions: pH = 5, sorbent dosage = 1 g/L, temperature = 25 ^{0}C]

3.3.3 Estimation of best fitting kinetic models

To quantitatively compare the applicability of each model, a normalised standard deviation (Δq) was calculated using Eq. (4):

$$\Delta q(\%) = 100x\sqrt{\frac{\sum\left[\left(q_{t,\exp} - q_{t,cal}\right)/q_{t,\exp}\right]^2}{n-1}} \quad (4)$$

where n is the number of data points, $q_{t,exp}$ and $q_{t,cal}$ are the experimental and calculated adsorption uptake at time t, respectively. The lower the value of normalized standard deviation, the more accurate is the model that predicts the experimental data. The aforesaid error analysis also has been applied to verify the kinetic model used to describe the heavy metal adsorption onto dried biomass of red seaweed Kappaphycus sp. from aqueous solutions and the biosorption of U(VI) from aqueous systems by malt spent rootlets, respectively [25,26].

3.3.4 Comparison between kinetic models

A relatively high R^2 value indicates that the model successfully describes the sorption kinetics. It was noticed from Table 3 that the pseudo-second-order kinetic equation can adequately describe the kinetic process of heavy metals sorption onto the zirconium-based magnetic sorbent as the correlation coefficients obtained by pseudo-second-order showed good linearity. The data suggested that the pseudo-second-order adsorption behaviour dominated the sorption process, and the adsorption rates of heavy metals onto the sorbents were probably controlled by the chemical process. Moreover, the calculated q_e values also agree perfectly with the experimental data in the case of pseudo-second-order kinetics. Correlation coefficients obtained adequately fitted well for all models but the ranking was in the order of pseudo-second-order > Weber-Morris diffusion.

On the other hand, the validity of the two kinetic models was revised and the normalized standard deviation obtained for each model was listed in Table 3. The Weber-Morris diffusion model has validated the surface adsorption and intra-particle diffusion operated concurrently during sorbent and adsorbate interaction. As presented in Table 3, Δq for Weber-Morris diffusion kinetic model are low (all less than 10.01%), followed by those of pseudo-second-order kinetic model (all less than 16.65%). Subsequently, the sorption process of the heavy metal ions by the zirconium-based magnetic sorbent could be better depicted by the pseudo-second-order kinetic model for all the studied initial metal ion concentrations except for the Cd^{2+} at high concentration (100 mg/L) which is better described by the Weber-Morris diffusion kinetic model. This may be due to the initial faster mass transfer of abundant cadmium ions through the boundary layer and adsorption on the sorbent surface, followed by slow diffusion inside the particles. It was the internal diffusion which determined the adsorption rate of the liquid system [27].

A number of researchers have studied the removal of metal ions onto various magnetic sorbents and reported that such studies mostly followed pseudo-second-order kinetic. Zhang et al. [28] pointed out that the kinetics of arsenic adsorption onto co-precipitated bimetal oxide magnetic nanomaterials fit well with the pseudo-second-order kinetic model. A study by Lin et al. [29] also claimed that the adsorption kinetics was well described by the pseudo-second-

order equation for all systems studied for the extraction and recycling utilization of metal ions with magnetic polymer beads, indicating that the chemical sorption was controlled by the rate-limiting step and not involved a mass transfer in solution. In the same manner, Tan et al. [30] has reported that the adsorption of Pb^{2+} by amino-functionalized Fe_3O_4 magnetic nano-particles obeyed the pseudo-second order kinetic model better than the Elovich and intra-particle diffusion models for its higher correlation coefficients.

Table 3 - The comparison between correlation coefficient, R^2 and normalized standard deviation (Δq) among two kinetic models

Kinetic Models	Copper (Cu)						Zinc (Zn)						Cadmium (Cd)					
	20 mg/L		50 mg/L		100 mg/L		20 mg/L		50 mg/L		100 mg/L		20 mg/L		50 mg/L		100 mg/L	
	R^2	Δq (%)	R^2	Δq (%)	R^2	Δq (%)	R^2	Δq (%)	R^2	Δq (%)	R^2	Δq (%)	R^2	Δq (%)	R^2	Δq (%)	R^2	Δq (%)
Pseudo-second-order	0.994	0.16	0.998	3.47	1.000	1.95	0.994	4.75	0.999	1.49	0.998	1.37	0.963	2.90	0.989	0.16	0.894	16.65
Weber-Morris diffusion	0.682	4.58	0.873	5.76	0.729	8.64	0.851	6.53	0.688	6.20	0.676	6.79	0.646	1.50	0.682	10.01	0.916	3.19

4. Conclusions

In the present study, the zirconium-based magnetic sorbent was synthesized through chemical co-precipitation of Fe^{2+} and Fe^{3+} in a zirconium sulfate solution. The removal of divalent metal ions, Cu^{2+}, Zn^{2+}, and Cd^{2+} was studied using the sorbent. The sorption rate was increased with an increase in contact time and initial metal ion concentration. A two-stage kinetics behaviour, which composed of a fast initial removal (in the first 60 min of treatment) and a slower subsequent removal up to equilibrium state which was obtained within 240 min of treatment, was observed. All the batch experiments achieved equilibrium state within 4 hours. Under comparable conditions, the amount of sorption decreased in the order of $Cu^{2+} > Cd^{2+} > Zn^{2+}$.Instrumental analyses to characterize the magnetic sorbent were performed using Fourier Transform InfraRed (FT-IR) Spectroscopy, Scanning Electron Microscopy (SEM), and Brunauer, Emmett, and Teller (BET) surface area analyser to investigate the factors that influence the sorption process. From the FT-IR analysis, the experimental data was corresponded to the peak changes of the spectra obtained before and after sorption process where -OH groups played an important role in the process. Studies on SEM demonstrated the existence of Cu^{2+}, Zn^{2+}, and Cd^{2+} on the sorbent surface after the sorption process. The BET surface area and porosity analysis has shown a distinct decrease of the surface area besides average pore radius and total pore volumes of the microporous sorbent after sorption process. The effects of contact time and initial metal ion concentration on the sorption process were evaluated using two adsorption kinetic models, namely pseudo-second-order and Weber-Morris diffusion. Based on the evaluation of the correlation coefficient (R^2) and normalized standard deviation, Δq (%), pseudo-second order and Weber-Morris diffusion model was proved to govern the adsorption rate. It also indicated that the sorption was chemical adsorption process and intra-particle diffusion operated simultaneously during sorbent and adsorbate interaction especially for Cd^{2+} at high concentration (100 mg/L). The kinetic experimental data proved that the zirconium-based magnetic sorbent synthesized in this study could be successfully applied for adsorbing metal ions and removing heavy metal divalent ions from aqueous solution. The magnetic sorbent has a great potential for the application in controlling the heavy metal contamination exists in aqueous waste streams of many industries.

Acknowledgement

The author would like to acknowledge the Universiti Malaysia Sarawak, Kota Samarahan, Mahsa University, Jenjarom, and Oriental Institute of Science and Technology, Bhopal.

References

[1] Sutherland,D.L. & Ralph, P.J. (2019). Microalgal bioremediation of emerging contaminants - Opportunities and challenges. *Water Research*, Volume 164, 1 November 2019, Article 114921

[2] Lee, Z.S., Chin, S.Y., Lim, J.W., Witoon, T. & Cheng, C.K. (2019). Treatment technologies of palm oil mill effluent (POME) and olive mill wastewater (OMW): A brief review. *Environmental Technology & Innovation*, Volume 15, August 2019, Article 100377

[3] Malakar, S., Saha, P.D., Baskaran, D. & Rajamanickam, R. (2019). Comparative study of biofiltration process for treatment of VOCs emission from petroleum refinery wastewater—A review. *Environmental Technology & Innovation*, Volume 8, November 2017, Pages 441-461

[4] Chu, W.L., Dang, N.L., Kok, Y.Y., Yap, K.S.I. & Convey, P. (2019). Heavy metal pollution in Antarctica and its potential impacts on algae. *Polar Science*, Volume 20, Part 1, June 2019, Pages 75-83

[5] Ashraf, S., Ali, Q., Zahir, Z.A., Ashraf, S. & Asghar, H.N. (2019). Phytoremediation: Environmentally sustainable way for reclamation of heavy metal polluted soils. *Ecotoxicology and Environmental Safety*, Volume 174, 15 June 2019, Pages 714-727

[6] Zhu, Y., Fan, W., Zhou, T. & Li, X. (2019). Removal of chelated heavy metals from aqueous solution: A review of current methods and mechanisms. *Science of The Total Environment*, Volume 678, 15 August 2019, Pages 253-266

[7] Haddaway, N.R., McConville, J. & Piniewski, M. (2018). How is the term 'ecotechnology' used in the research literature? A systematic review with thematic synthesis. *Ecohydrology & Hydrobiology*, Volume 18, Issue 3, July 2018, Pages 247-261

[8] Singh, N. B., Nagpal, G., Agrawal & S., Rachna (2018). Water purification by using Adsorbents: A Review *Environmental Technology & Innovation*, Volume 11, August 2018, Pages 187-240

[9] Takafuji, M., Ide, S., Ihara, H. & Xu, Z.H. (2004). Preparation of poly(1-vinylimidazole)-grafted magnetic nanoparticles and their application for removal of metal ions. *Chemistry of Materials*, 16, 1977-1983.

[10] Gong, J., Chen, L., Zeng, G., Long, F., Deng, J., Niu, Q., & He, X. (2012). Shellac-coated iron oxide nanoparticles for removal of cadmium(II) ions from aqueous solution. *Journal of Environmental Sciences (China)*, 24(7), 1165-1173.

[11] Liu, W., Zhao, X., Wang, T., Fu, J. & Ni, J.R. (2015). Selective and irreversible adsorption of mercury(II) from aqueous solution by a flower-like titanate nanomaterial. *Journal of Materials Chemistry A*, 3, 17676-17684.

[12] Lim, S.F. (2008). *Adsorption of Contaminations by Magnetic Sorbents*. Ph.D. Thesis. Department of Chemical and Biomolecular Engineering, National University of Singapore, Singapore.

[13] Zheng, Y.M., Lim, S.F. & Chen, J.P. (2009). Preparation and characterization of zirconium-based magnetic sorbent for arsenate removal. *Journal of Colloid and Interface Science*, 338(1), 22-29.

[14] Arshadi, M., Amiri, M.J. & Mousavi, S. (2014). Kinetic, equilibrium and thermodynamic investigations of Ni(II), Cd(II), Cu(II) and Co(II) adsorption on barley straw ash. *Water Resources and Industry*, 6, 1-17.

[15] Mphahlele, K., Onyango, M.S. & Mhlanga, S.D. (2015). Kinetics, equilibrium, and thermodynamics of the sorption of bisphenol A onto n-CNTs-β-cyclodextrin and Fe/N-CNTs-β-cyclodextrin nanocomposites. *Journal of Nanomaterials*, 2015, 1-13.

[16] Sajidu, S.M.I., Persson, I., Masamba, W.R.L., Henry, E.M.T. & Kayambazinthu, D. (2006). Removal of Cd^{2+}, Cr^{3+}, Cu^{2+}, Hg^{2+}, Pb^{2+} and Zn^{2+} cations and AsO_4^{3-} anions from aqueous solutions by mixed clay from Tundulu in Malawi and characterisation of the clay. *Water S.A*, 32(4), 519-526.

[17] Bouraada, M., Ouali, M.S. & de Ménorval, L.C. (2012). Dodecylsulfate and dodecybenzenesulfonate intercalated hydrotalcites as adsorbent materials for the removal of BBR acid dye from aqueous solutions. *Journal of Saudi Chemical Society*, 20(4), 397-404.

[18] Ossman, M.E. & Mansour, M.S. (2013). Removal of Cd(II) ion from wastewater by adsorption onto treated old newspaper: Kinetic modeling and isotherm studies. *International Journal of Industrial Chemistry*, 4(13), 1-7.

[19] Soni, A., Tiwari, A. & Bajpai, A.K. (2012). Adsorption of o-nitrophenol onto nano iron oxide and alginate microspheres: Batch and column studies. *African Journal of Pure and Applied Chemistry*, 6(12), 161-173.

[20] Pereira, F.J., Díez, M.T. & Aller, A.J. (2015). Effect of temperature on the crystallinity, size and fluorescent properties of zirconia-based nanoparticles. *Materials Chemistry and Physics*, 152, 135-146.

[21] Gromadskaya, L.I., Romanova, I.V., Vyshnevskyi, O.A. & Kirillov, S.A. (2013). Near-stoichiometric adsorption of phosphate by silica gel supported nanosized hematite. *ISRN Inorganic Chemistry*, 2013, 1-10.

[22] Kyzas, G.Z. & Bikiaris, D.N. (2015). Recent modifications of chitosan for adsorption applications: A critical and systematic review. *Marine Drugs*, 13(1), 312-337.

[23] Zainol Abidin, N. A., Palaniandy, P., Yusoff, M.S. & Amr, S.S.A. (2019). Activated Carbon-Limestone-Alginate Beads for the Simultaneous Removal of Color and Turbidity of Kerian River. International Journal of Integrated Engineering, 11(2). Retrieved from https://publisher.uthm.edu.my/ojs/index.php/ijie/article/view/4118

[24] Maksin, D.D., Kljajević, S.O., Đolić, M.B., Marković, J.P., Ekmeščić, B.M., Onjia, A.E. & Nastasović, A.B. (2012). Kinetic modeling of heavy metal sorption by vinyl pyridine-based copolymer. *Hemijska Industrija*, 66(6), 795-804.

[25] Rahman, M.S. & Sathasivam, K.V. (2015). Heavy metal adsorption onto Kappaphycus sp. from aqueous solutions: The use of error functions for validation of isotherm and kinetics models. *BioMed Research International*, 2015, 1-13.

[26] Anagnostopoulos, V., Symeopoulos, B., Bourikas, K. & Bekatorou, A. (2016). Biosorption of U(VI) from aqueous systems by malt spent rootlets. Kinetic, equilibrium and speciation studies. *International Journal of Environmental Science and Technology*, 13, 285-296.

[27] Moon, W. C. & Palaniandy, P. (2019). A Review on Interesting Properties of Chicken Feather as Low-Cost Adsorbent. International Journal of Integrated Engineering, 11(2). Retrieved from https://publisher.uthm.edu.my/ojs/index.php/ijie/article/view/4247

[28] Zhang, S.X., Niu, H.Y., Cai, Y.Q., Zhao, X.L. & Shi, Y.L. (2010). Arsenite and arsenate adsorption on coprecipitated bimetal oxide magnetic nanomaterials: $MnFe_2O_4$ and $CoFe_2O_4$. *Chemical Engineering Journal*, 158, 599-607.

[29] Lin, Z.Y., Zhang, Y.X., Chen, Y.L. & Qian, H. (2012). Extraction and recycling utilization of metal ions (Cu^{2+}, Co^{2+} and Ni^{2+}) with magnetic polymer beads. *Chemical Engineering Journal*, 200-202, 104-112.

[30] Tan, Y.Q., Chen, M. & Hao, Y.M. (2012). High efficient removal of Pb (II) by amino-functionalized Fe_3O_4 magnetic nano-particles. *Chemical Engineering Journal*, 191, 104-111.